Chemical Engineering Journal 493 (2024) 152772

Contents lists available at ScienceDirect

Chemical Engineering Journal

journal homepage: www.elsevier.com/locate/cej

Assessing the Long-Term performance of an integrated microbial fuel Cell-Anaerobic membrane bioreactor for swine wastewater treatment

Haojie Huang [a,b], Xinbo Zhang [a,b,*], Qing Du [a,b], Fu Gao [a,b], Zhiwen Wang [c], Guangxue Wu [d], Wenshan Guo [a,e], Huu Hao Ngo [a,e,**]

[a] Joint Research Centre for Protective Infrastructure Technology and Environmental Green Bioprocess, School of Environmental and Municipal Engineering, Tianjin Chengjian University, Tianjin 300384, China

[b] Tianjin Key Laboratory of Aquatic Science and Technology, Tianjin Chengjian University, Jinjing Road 26, Tianjin 300384, China

[c] Frontier Science Center for Synthetic Biology and Key Laboratory of Systems Bioengineering (Ministry of Education), SynBio Research Platform, Collaborative Innovation Center of Chemical Science and Engineering (Tianjin), Department of Biochemical Engineering, School of Chemical Engineering and Technology, Tianjin University, Tianjin 300072, China

[d] Civil Engineering, School of Engineering, College of Science and Engineering, University of Galway, Galway H91 TK33, Ireland

[e] Centre for Technology in Water and Wastewater, School of Civil and Environmental Engineering, University of Technology Sydney, Sydney, NSW 2007, Australia

ARTICLE INFO

Keywords:
Microbial fuel cell
Anaerobic membrane bioreactor
Swine wastewater
Membrane fouling
Microbial analyses

ABSTRACT

To improve the performance of an anaerobic membrane bioreactor (AnMBR) treating swine wastewater, an integrated microbial fuel cell (MFC)-AnMBR was constructed and operated for 185 days at organic concentrations of 3000—12000 mg/L to investigate the effect of the in-situ bioelectric field on organic removal, methane production, system stability and membrane fouling. Results showed that MFC-AnMBR achieved up to 99.0 % chemical oxygen demand (COD) removal at all organic loads with the maximum methanogenic capacity of 0.21 L/gCODremoved. Compared to conventional AnMBR, MFC-AnMBR shortened the start-up period by 15 days, improved the COD removal by 8.7 ± 1.5 % and methane production by 54.2 ± 37.8 %. In the presence of the bioelectric field, the concentrations of soluble microbial products (SMP) and extracellular polymeric substances (EPS) were reduced by 52.7 ± 10.9 % and 15.7 ± 10.9 %, respectively. Notably, the bioelectric field extended the membrane life cycle by more than 40 days. Facilitated by the bioelectric field, the abundance of g_Methanothrix and g_Brooklawnia (capable of electron transfer with g_Methanothrix) in MFC-AnMBR were increased by 29.5 % – 48.7 % and 8.2 % – 10.8 %, respectively, greatly enhancing the methanogenic performance. Furthermore, the bioelectric field inhibited the growth of membrane-fouling bacteria (p_Bacteroidota and p_Firmicutes) and promoted the proliferation of membrane-fouling-mitigating bacteria p_Actinobacteria on the membranes. Overall, the integrated MFC-AnMBR system exhibited an excellent long-term operation performance when treating swine wastewater at different organic loads. This provided a promising strategy for stabilising and efficiently treating swine wastewater.

Abbreviations: AnMBR, Anaerobic membrane bioreactor; SW, swine wastewater; COD, chemical oxygen demand; BES, bioelectrochemical systems; MFC, microbial fuel cell; MEC, microbial electrolysis cell; SRT, sludge retention time; HRT, hydraulic retention time; SMP, soluble microbial product; EPS, extracellular polymeric substance; TMP, transmembrane pressure; MLSS, mixed liquor suspended solids; MLVSS, mixed liquid volatile suspensions; CV, cyclic voltammetry; CE, coulomb efficiency; DNA, deoxyribonucleic acid; pH, potential of hydrogen; VFAs, volatile fatty acids; F/M, food/microorganism; PN/PS, protein/polysaccharide; DIET, direct interspecies electron transfer.

* Correspondence authors at: Joint Research Centre for Protective Infrastructure Technology and Environmental Green Bioprocess, School of Environmental and Municipal Engineering, Tianjin Chengjian University, Tianjin 300384, China.

** Correspondence authors at: Joint Research Centre for Protective Infrastructure Technology and Environmental Green Bioprocess, School of Environmental and Municipal Engineering, Tianjin Chengjian University, Tianjin 300384, China.

E-mail addresses: zxbcj2006@126.com (X. Zhang), ngohuuhao121@gmail.com (H. Hao Ngo).

https://doi.org/10.1016/j.cej.2024.152772
Received 3 March 2024; Received in revised form 31 May 2024; Accepted 1 June 2024
Available online 2 June 2024

1. Introduction

With the rapid development of pig farming, its induced environmental problems have become increasingly prominent. As the world's largest pig breeder, about 726.62 million pigs were slaughtered and 57.94 million tons of pork were produced in China (China Statistical Yearbook, 2023), with the generated swine wastewater (SW) up to 1,061——2,122 million tons [1]. The mixed SW contains a large number of organic matters, solids, volatile substances, bacterial flora and harmful substances (antibiotics, heavy metals, etc.), with the chemical oxygen demand (COD) between 2000——30000 mg/L, ammonium nitrogen between 110——1650 mg/L, total nitrogen between 200——2050 mg/L, and total phosphorus between 100——620 mg/L [2]. If not effectively treated, the discharge of SW would cause serious environmental problems in receiving water bodies.

Approaches commonly applied to treat SW include physicochemical technologies (advanced oxidation, flocculation, etc.), natural degradation systems (oxidation ponds, artificial wetlands, etc.) and biological technologies (aerobic digestion, anaerobic digestion, etc.). Considering the high organic contents in SW, anaerobic digestion can effectively remove pollutants and recover energy, a sustainable and environmentally friendly technology [3–5]. In recent years, anaerobic membrane bioreactor (AnMBR) have been used to treat different types of high-concentration organic wastewater due to their perfect pollutant removal and efficient biogas production. Thanks to membrane retention, AnMBR can efficiently maintain high biomass concentration within the reactor, achieve high effluent quality and remove emerging pollutants [6]. In addition, the complete separation of sludge retention time (SRT) and hydraulic retention time (HRT) in AnMBR avoids microbial washout and can effectively retain slow-growing functional microorganisms (e.g. methanogens) in the reactor, promoting system stability and methane production [7]. Such as, Liu et al. applied AnMBR to treat SW with an organic load of 4.4——8.7 mg/(L·d) and achieved 93 % − 98 % COD removal and 0.22——0.28 L/gCOD methane production [8]. Zhang et al. obtained 96 % − 98 % COD removal and 0.43 ± 0.04 L/gCOD biogas production when treating SW with an organic load of about 2.4 mg/(L·d) [9].

AnMBR can effectively improve digestion performance, but there are still some challenges in treating SW. High concentrations of ammonia, antibiotics, and heavy metals in SW not only inhibit microbial activity and cause a decrease in methanogenesis but also increase membrane pollutants (soluble microbial product (SMP) and extracellular polymeric substance (EPS)), thus exacerbating membrane fouling [10]. For instance, Cheng et al. observed a dramatic increase in the transmembrane pressure (TMP) from 3 to 25 kPa within 8 days, indicating severe membrane fouling during AnMBR operation for SW treatment [11–13].

As well known, operating parameters, sludge characteristics and microbial community influence membrane fouling [14,15]. To optimize the treatment of SW by AnMBR and alleviate membrane fouling, various strategies have been proposed, including physicochemical flushing, introduction of functional additives and bioelectrochemical systems (BES) [10,16–19]. Among them, BES is a promising new technology for wastewater treatment, which can convert organic matters into electricity in microbial fuel cell (MFC) or hydrogen in microbial electrolysis cell (MEC) by exoelectrogens [20,21]. Furthermore, introducing BES into AnMBR, especially MFC, has received intensive attention due to its ability to control membrane fouling and improve system performance [13,16,20,22]. Liu et al. coupled MFC with AnMBR to remove membrane pollutants and found the system reduced the membrane surface proteins, α-polysaccharides and β-polysaccharides by 45.34 %, 57.19 % and 26.46 %, respectively, and prolonged the membrane fouling cycle by 89 days [22]. Hao et al. designed an integrated MFC-AnMBR system to treat SW, which exhibited a 35.9 % increase in methane production and a decrease in the production of SMP and EPS by 65.3 % and 43.1 % [16]. Therefore, the introduction of MFC would mitigate membrane fouling in AnMBR and enhance system performance.

At present, there are few studies on the treatment of swine wastewater by the MFC-AnMBR system, so there is a need to continue to carry out related research. In our previous work, an integrated MFC-AnMBR system was built by involving an AnMBR and a single chamber air–cathode MFC in a typical reaction chamber and successfully started for SW treatment [16]. The system achieved high methane production and a short start-up phase, but the treatment and long-term performance of high concentrations of SW still need to be further investigated. As such, this study employed an integrated MFC-AnMBR system to treat SW with different organic loads and explore the potential mechanisms in-situ enhancement of AnMBR by bioelectric fields under long-term operation, including treatment efficacy, methane production, membrane fouling control, and microbial communities. This study evaluates the feasibility of the MFC-AnMBR system to treat SW and provides theoretical support for large-scale and low-cost SW treatment.

2. Materials and methods

2.1. Operation of the integrated system

The reactor was plexiglass with an inner diameter of 130 mm, a height of 315 mm and a practical work volume of 2.0 L (Fig. 1). The temperature was maintained by a circulating thermostatic water bath (Bilang Experimental Instrument Manufacturing Co. Ltd, Wuxi, China). The membrane module was a polyvinylidene fluoride hollow fiber membrane (Haike Membrane Technology Co. Ltd, China) with a pore size of 0.1 μm. A pressure sensor (MBS1900, Danfoss, Denmark) and a paperless recorder (BRW500 − 5100, Fü rest) were connected to the effluent section of the membrane module to measure the TMP. The biogas was collected using aluminum foil bags.

During the operation, wastewater enters from the reactor bottom and filters out through the membrane after treatment, with the influent and effluent controlled by peristaltic pumps. Some generated biogas was used in the self-circulation process to mix the sludge and wastewater; the detailed operation referred to our previous study [11].

The systems were operated continuously for 185 days. Both systems adopted a continuous flow operation under the same influent conditions. The experiment was divided into 5 phases depending on the influent COD concentration, as shown in Table 1.

2.2. Materials and chemicals

The inoculated sludge was taken from an anaerobic digester in a wastewater treatment plant in Tianjin. The inoculated sludge's concentration of mixed liquor suspended solids (MLSS) was 40,000 mg/L, and 500 mL inoculated sludge was added into the reactors for system start-up. The synthetic SW contained $C_6H_{12}O_6$ (3000——12000 mg/L), NH_4Cl (120——480 mg/L), KH_2PO_4 (120——480 mg/L), $FeCl_2$ (112 mg/L), $MgSO_4$ (30 mg/L) and small amounts of essential trace elements. The essential trace elements included $MnCl_2$ (1 mg/L), $ZnCl_2$ (1 mg/L), $NiCl_2$ (21 mg/L), $CoCl_2$ (13 mg/L), $CuCl_2$ (0.25 mg/L), H_3BO_3 (0.05 mg/L), and Na_2MoO_4 (0.24 mg/L) [16].

2.3. Analysis methods

COD was detected by potassium dichromate rapid digestion spectrophotometry; potential of hydrogen (pH) was detected using a pH meter (HACH HQ11D, USA) [9]. Biogas components were analyzed by gas chromatography (GC-2014, Shimadzu, Japan). The gravimetric method determined MLSS and mixed liquid volatile suspensions (MLVSS) [23]. SMP and EPS were analyzed according to the method used in the research [16]. Polysaccharides and proteins were analyzed using phenol–sulfuric acid and Forint-Ciocalteu methods [24]. Sludge particle size and zeta potential were determined using a Malvern laser particle size analyzer (Malvern Masters Sizer 2000, Malvern

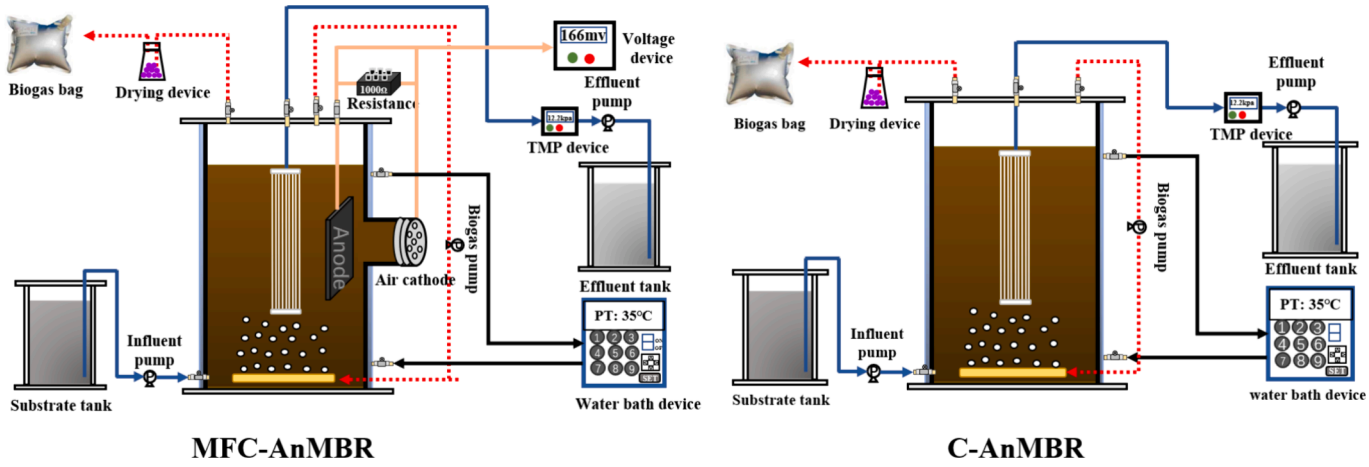

Fig. 1. The diagram of the two sets of devices.

Table 1
Operation parameters of the AnMBR systems.

Experimental Phases	COD concentration (mg/L)	HRT (h)	Operating temperature (℃)	Operation time (d)
Phase 1	3200 ± 200	96	35 ± 1	57
Phase 2	5300 ± 200			41
Phase 3	7500 ± 200			20
Phase 4	9600 ± 200			27
Phase 5	11700 ± 200			40

Instruments, UK) and a zeta potential analyzer.

Electrochemical parameters were measured for MFC-AnMBR. Cell voltages were collected every 30 min by clicking a data acquisition card (DAM-3000 m, Beijing Altai Technology Co., Ltd.). Cyclic voltammetry (CV) was measured using an electrochemical potentiometer (Shanghai Chenhua Instruments Co., Ltd., China). The polarization curves were analyzed using the steady-state discharge method. The coulomb efficiency (CE) was calculated as the actual electron recovery rate and the theoretical power generation of the substrate by the following equation (1) [16]:

$$CE = 32\Sigma_{i=1}^{n} U_i \cdot t_i / RFbv\Delta COD \quad (1)$$

where: U is the voltage output at time t, R is the resistance value, F is the Faraday constant (96,485C mol^{-1}) and b is the number of electrons produced theoretically per consumption of 1 mol COD.

2.4. Microbial community analysis

At the end of each phase, the sludge samples were analyzed using 16S rRNA sequencing to evaluate the changes in the microbial community. The biomass on the membrane was collected for analysis in Phase 3, as membrane replacement occurred in Phase 2.

Deoxyribonucleic acid (DNA) was extracted using the E.Z.N.A.® soil kit (Omega Bio TEK, Norcross, GA, USA). The concentration and purity of DNA were detected by Nanodrop 2000, and the quality of DNA extraction was confirmed by 1.0 % agarose gel electrophoresis. PCR amplification of the variable region of colony V3 − V4 was conducted with primers 515F (GTGCCAGCMGCCGCGG) and 806R (GGACTACHVGGGTWTCTAAT). The PCR products were detected and quantified using QuantiFluor™-ST (Promega, USA) and then sequenced on Illumina's Miseq PE300 platform from Illumina (commissioned by Shanghai Meiji Biomedical Technology Co., Ltd.). Raw sequences were quality-controlled using the Trimmomatic software, spliced using the FLASH software [25] and clustered using the UPARSE software [26] (version 7.1) based on 97.0 % similarity to OTU. In the meantime, single sequences and chimeras were removed during clustering. Each line was annotated with species classification using the RDP classifier [27], compared to the Silva database (SSU123), and a comparison threshold of 70.0 % was established.

3. Results and discussion

3.1. Electrochemical characteristics of MFC-AnMBR

3.1.1. The voltage, power density and CE curve

The voltage and power density visually reflected the stability and variability of MFC (Fig. 2a-b). During Phase 1, the voltage steadily rose from 93 mV to 160 mV, with a parallel rise in power density from 2.16 mW/m^2 to 6.40 mW/m^2. Phase 1 was a crucial start-up phase for MFC, and the voltage continuously increased slowly. During this period, the biofilm on the anode carbon grew and matured, transferring electrons from microbial respiration to the anode more efficiently. The start-up phase of MFC spanned approximately 50 days. Afterwards, the voltage and power density reached their maximum values simultaneously and remained stable at 160 mV and 6.40 mW/m^2, respectively. Subsequently, in Phase 2 to Phase 5, sustained stability in both voltage and power density was obtained, with only minor fluctuations occurring. The voltage averaged 150 ± 10 mV, and the power density remained at 5.68 ± 0.81 mW/m^2. These slight fluctuations in voltage, particularly following an increase in organic load, could be due to the adaptation of electroactive bacteria to changes in organic load and the competitive interactions with other microorganisms. Interestingly, it was notable that the voltage and power density did not rise with increasing organic load.

As shown in Fig. 2b, the CE kept increasing steadily in Phase 1, indicating that the utilization of the substrate by electroactive bacteria kept growing. In MFC-AnMBR, the CE relied on the dynamic competition for substrates between electroactive and non-electroactive bacteria, such as fermenters and methanogens, especially during the start-up phase or when organic concentration was scarce. However, the CE did not rise with increasing organic loads in sucessive phases, indicating that these two parameters were not correlated. Calculations concerning organic engagement and CE revealed that electroactive bacteria consistently consumed approximately 90 ± 10 mg/L of substrate for electricity generation from Phase 1 (stabilization) to Phase 5. These findings strongly suggested that the biofilm formed on the anodic carbon felt reached a mature state during Phase 1 (stabilization), characterized by the peak rates of exoelectrogen reproduction, metabolism, and substrate consumption for efficient electron transfer [16]. Hence, it can be reasonably presumed that once the integrated system was successfully

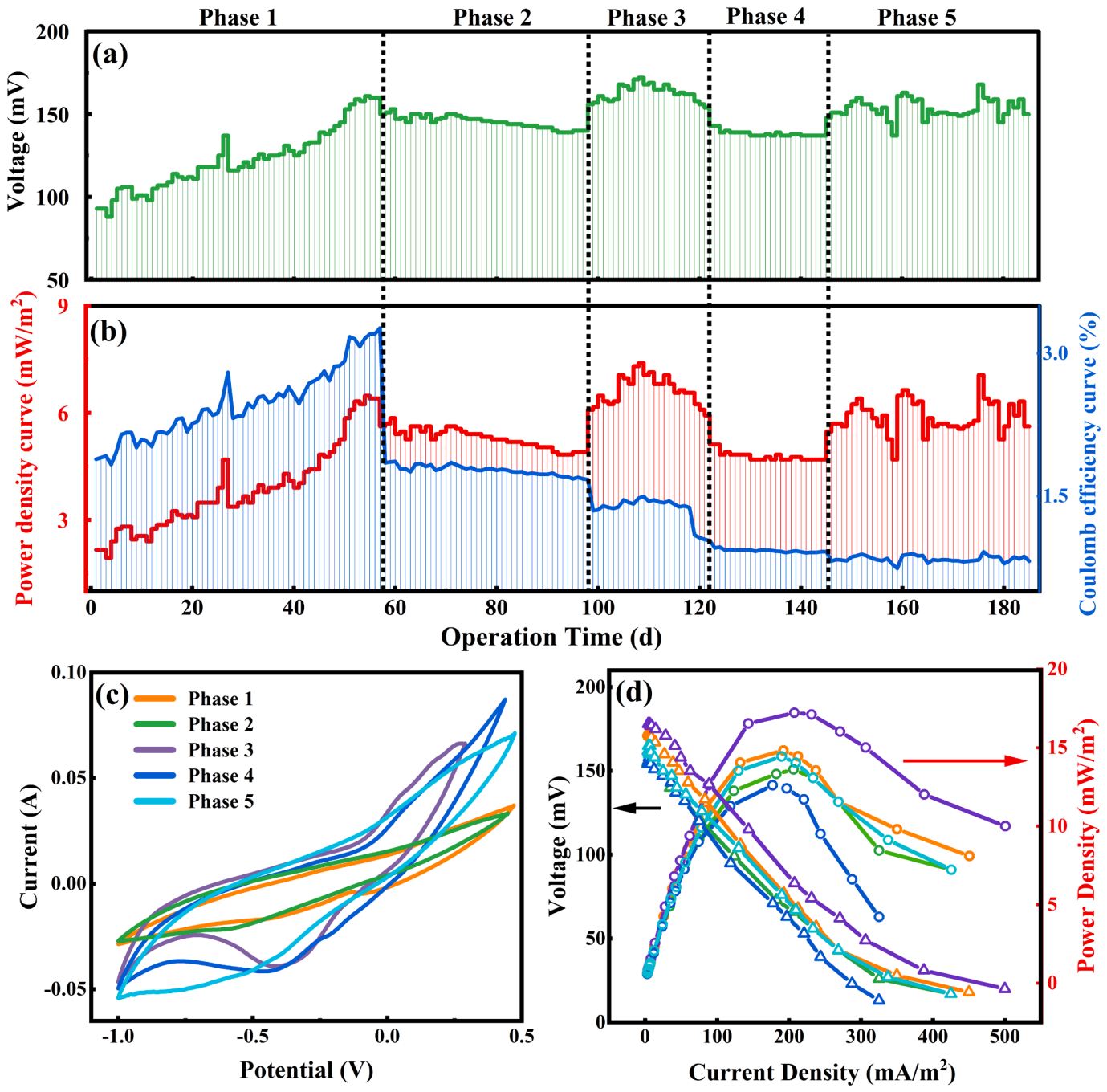

Fig. 2. Variations in (a) voltage, (b) power density and CE, (c) CV and (d) polarization curves of MFC-AnMBR.

started up and the organic concentration was sufficient, the primary factors influencing the CE were the intrinsic properties of the MFC system itself, including carbon fiber mats, electrochemical losses, and other relevant components.

3.1.2. *CV curve and polarization curve*

The CV curve's area gradually rose with reactor operation (increasing organic loads), and more pronounced redox peaks appeared (Fig. 2c). The size of the CV curve was positively correlated with the charging and discharging capacity, and the appearance of redox peaks was related to electron transfer. This indicated that the electrochemical performance and electron transfer of MFC-AnMBR were greatly enhanced during the reactor's operation. However, the weakening of the redox peak in Phase 5 indicated that the high organic load inhibited electroactive bacteria and thus affected electron transfer.

The polarization curves are shown in Fig. 2d. The internal resistance was obtained by regression line fitting, where the internal resistance was the slope of the regression line of the polarisation curve [28]. In this work, the values obtained in different phases were 123 Ω, 110 Ω, 113 Ω, 124 Ω and 155 Ω, respectively. The internal resistance of MFC-AnMBR went up gradually with increasing organic concentrations, which may be due to the increased mass transfer and ohmic resistance [29]. The higher internal resistance in Phase 1 than in Phase 2 was probably because the biofilm on the anode was not fully developed.

3.2. Performance of the MFC-AnMBR system

3.2.1. Pollutants removal

As shown in Fig. 2a, both reactors demonstrated remarkable efficiency in treating SW, with COD removal consistently above 90.0 %. This signified the effectiveness of the AnMBR technology in addressing the challenges associated with treating complex SW. Delving into the details, C-AnMBR exhibited a notable fluctuation in COD removal from Phase 1 to Phase 4. The dynamics of an initial decrease and then increase could be due to the inhibitory effect of the organic load on anaerobic microorganisms [30], because microorganisms need to adapt to the altered environmental conditions, resulting in the observed variations.

In contrast, MFC-AnMBR displayed only minor fluctuations in Phases 1 and 2, which required less time to reach and maintain high levels of COD removal. Impressively, MFC-AnMBR was not only able to achieve and sustain high COD removal in a shorter start-up period (MFC-AnMBR achieved 99.0 % COD removal and stabilized after day 19, while C-AnMBR achieved 97.0 % COD removal and stabilized after day 34), but the high COD removal was also unaffected by subsequent organic load shocks compared to C-AnMBR. This could be facilitated by the bioelectric field, which enhanced electron transfer between microbial cells and sludge activity [16]. The result was expedited adaptation of the microbes to external changes, contributing to rapid stabilization of the system. Throughout the experiment, MFC-AnMBR consistently maintained an exceptional COD removal ranging between 96.3 % and 100 %, while C-AnMBR fluctuated between 91.5 % and 100 %. This was consistent with the findings of Tan et al., who found that the combination of MFC and AnMBR provided higher COD removal than conventional AnMBR [31]. This was perhaps due to the activities of electroactive bacteria and other bacteria stimulated by electricity or the effective degradation of the inhibitory compounds (e.g., volatile fatty acids), which enhanced COD removal [20,32]. These findings strongly suggested that bioelectric fields play a crucial role in accelerating the start-up of an AnMBR system, improving organic matter removal and maintaining system stability.

3.2.2. pH

The optimal pH range for methanogens is 6.8——7.2. An increase or decrease in pH can directly affect the anaerobic digestion [33]. The pH in C-AnMBR ranged from 5.9 – 8.0 and fluctuated considerably, with significant acidification occurring particularly in Phases 1——3, highlighting the challenges in maintaining stability within this system (Fig. 3b). The substantial pH fluctuations observed may be attributed to the characteristics of the start-up phase and increasing organic load. These findings underscored the importance of organic load management in ensuring the stable operation of the anaerobic system [34].

The pH levels in MFC-AnMBR remained remarkably stable at 6.9——7.4 throughout the experiment, indicating that the bioelectric field strengthened the activity of methanogens and facilitated the timely conversion of volatile fatty acids. The result was that the integrated system avoided acidification and promoted higher organic matter removal. Notably, pH levels in MFC-AnMBR also achieved a relatively stable state earlier during the start-up phase of Phase 1, suggesting that the presence of a bioelectric field contributed to the accelerated start-up of the anaerobic system. This early stability was one of the key factors contributing to the faster and more consistent increase in the COD removal rate observed in MFC-AnMBR compared to C-AnMBR in the initial stages of the experiment.

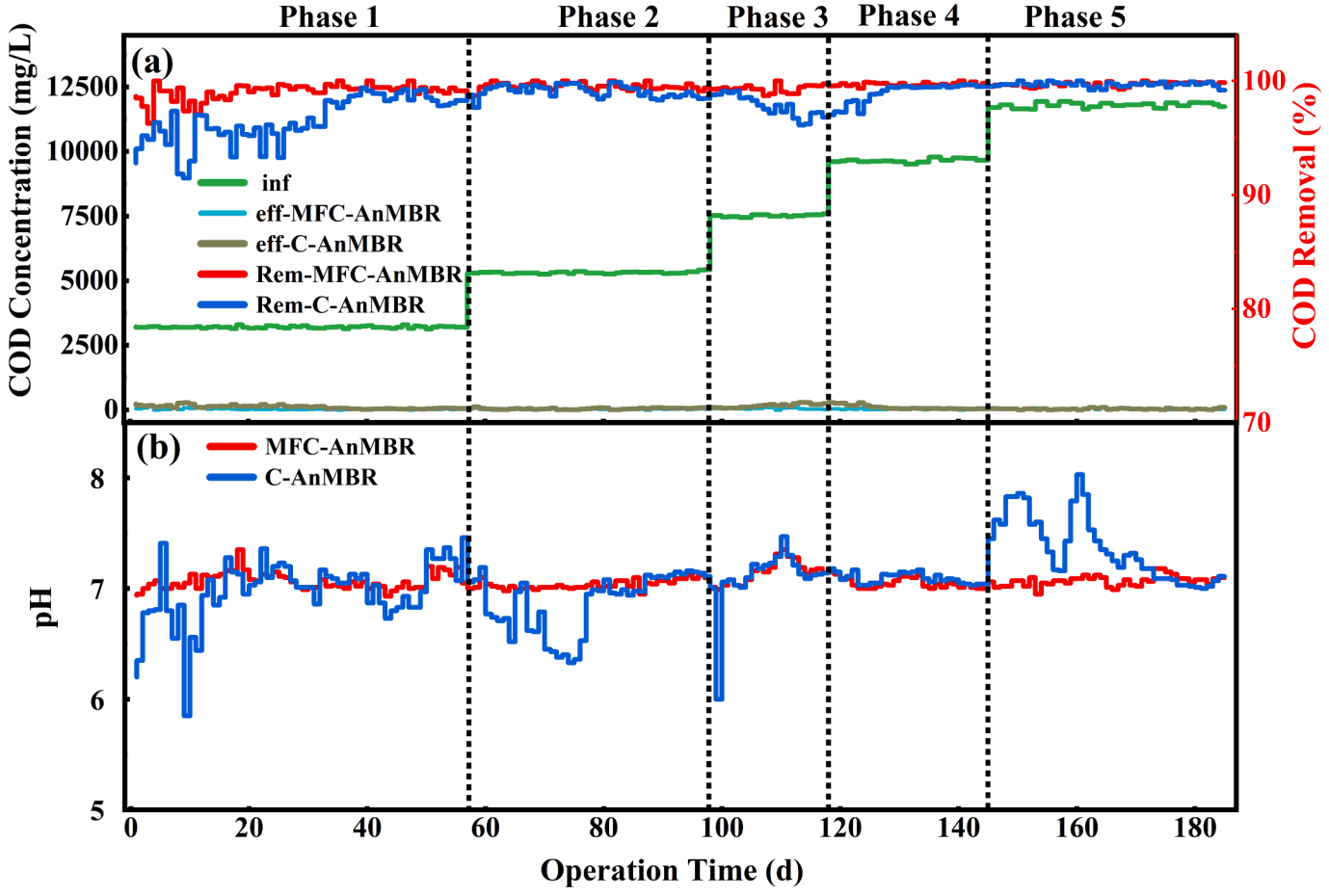

Fig. 3. Variations in (a) COD removal, (b) pH in C-AnMBR and MFC-AnMBR.

3.2.3. Methane production

The energy recovery was evaluated via the measurement of methane production and content (Fig. 4a-b). MFC-AnMBR consistently outperformed C-AnMBR in terms of methane production and methane content throughout the operation, Notably, the methane production and methane content in MFC-AnMBR showed a substantial upward trend right from Phase 1. In Phase 1, the methane production in MFC-AnMBR and C-AnMBR increased from 30 mL/d and 20 mL/d to 240 mL/d and 190 mL/d, respectively. Simultaneously, the methane content rose from 18.2 % and 14.5 % to 55.0 % and 47.2 %, respectively. This remarkable improvement can be attributed to the progressive enrichment of electroactive bacteria within MFC-AnMBR compared to C-AnMBR. As these electroactive bacteria multiplied, they generated an abundance of free electrons, enhancing the interactions between electroactive bacteria and non-electroactive bacteria, and consequently promoting the methanogenic process [16]. As a result, both methane production and methane content experienced significant increases in MFC-AnMBR. Furthermore, methane production and content continued to rise with increasing organic load. The increase in methane production was the fact that more Volatile Fatty Acids (VFAs) were available to the methanogens and promoted the proliferation of methanogens, generating more methane. The rise in methane content was associated with increased hydrogenotrophic methanogen *g_Methanobacterium* (*detailed in section 3.4*), which promoted the conversion of H_2 and CO_2 to methane in the biogas. In Phase 5, both methane production and methane content reached the maximum values of 1180 ± 35 mL/d and 71.0 ± 1.1 % in MFC-AnMBR, compared to about 890 ± 30 mL/d and 54.9 ± 2.8 % in C-AnMBR. Notably, the methanogenic performance in C-AnMBR showed significant fluctuations during Phases 2–5, suggesting that the high organic loading affected the anaerobic digestion process and methane

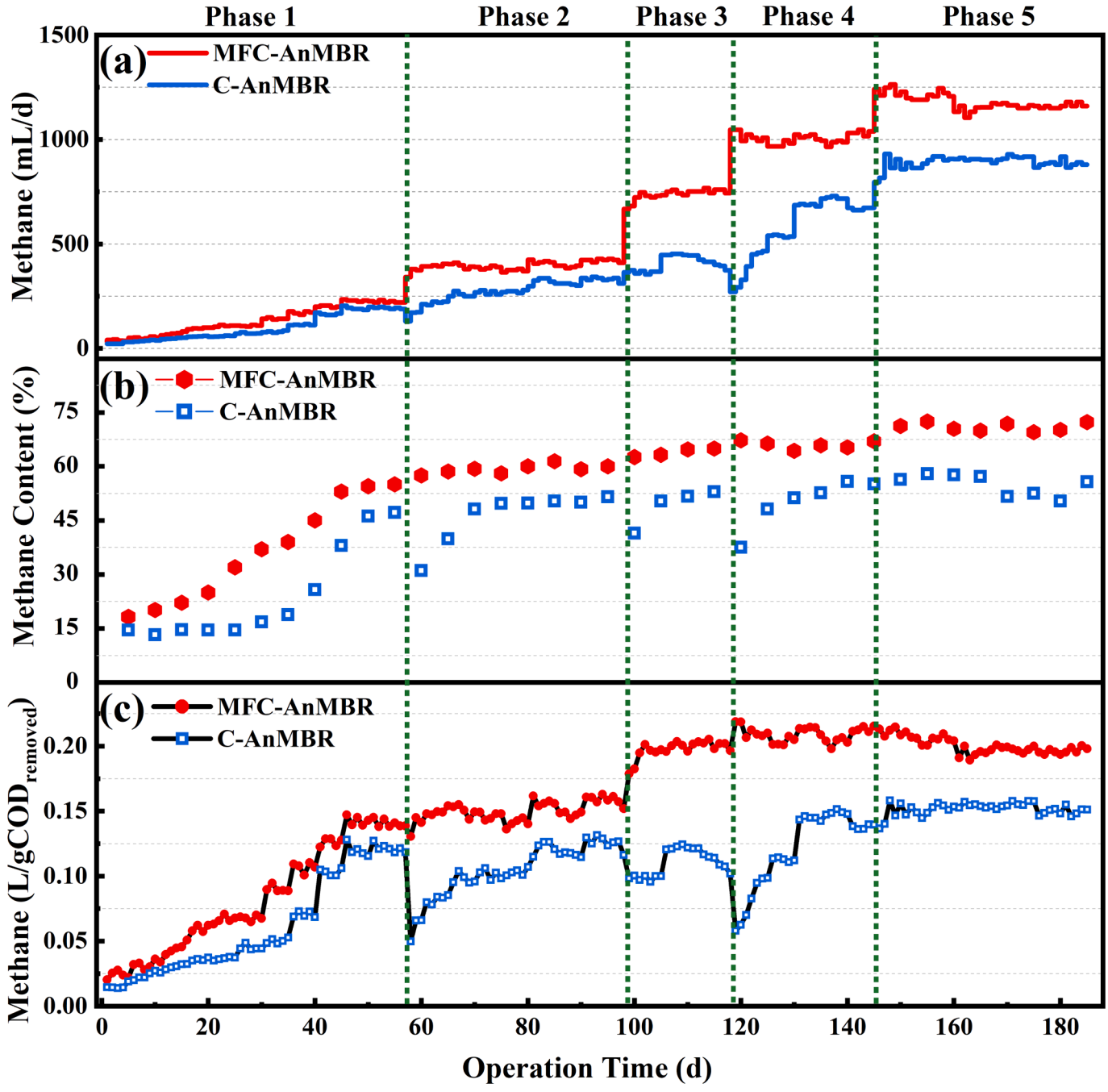

Fig. 4. Variations in (a) methane production, (b) methane content and (c) methane-producing ability in C-AnMBR and MFC-AnMBR.

production [30]. In contrast, the methanogenic performance in MFC-AnMBR was unaffected by high organic loads and exhibited a growing trend, suggesting that the bioelectric field enhanced the activity of anaerobic microorganisms, resulting in a more stable anaerobic digestion process and higher methane production efficiency [16].

Additionally, the methanogenic capacity was assessed by calculating methane production versus COD removal, as shown in Fig. 4c. The methanogenic capacity of the two systems rose gradually with increasing organic loads. However, it was clear that MFC-AnMBR possessed higher and more stable methanogenic capacity than C-AnMBR. This finding further demonstrated that the bioelectric field enhanced substrate utilization and methanogenic activity, resulting in higher and more stable methane production. In Phase 4, the methanogenic capacity of MFC-AnMBR peaked at 0.21 L/gCOD$_{removed}$, surpassing the performance of C-AnMBR at 0.14 L/gCOD$_{removed}$. This may be correlated with the optimal electrochemical performance in this phase, maximizing electron transfer between methanogens and electroactive bacteria (*detailed in section 3.1.2*).

3.2.4. Sludge characteristics

Fluctuations in MLSS and MLVSS were measured to determine the effect of changes in biomass on biological treatment (Fig. 5a-b). In Phases 1 and 2, MLSS and MLVSS concentrations in both reactors increased with increasing organic load. In Phases 3 and 4, MLSS and MLVSS in MFC-AnMBR were still growing, whereas those in C-AnMBR suddenly decreased by 13.0 %. Generally, higher food/microorganism (F/M) ratios resulted in more available substrates with higher organic loads, which could support the rapid microbial growth [35], consistent

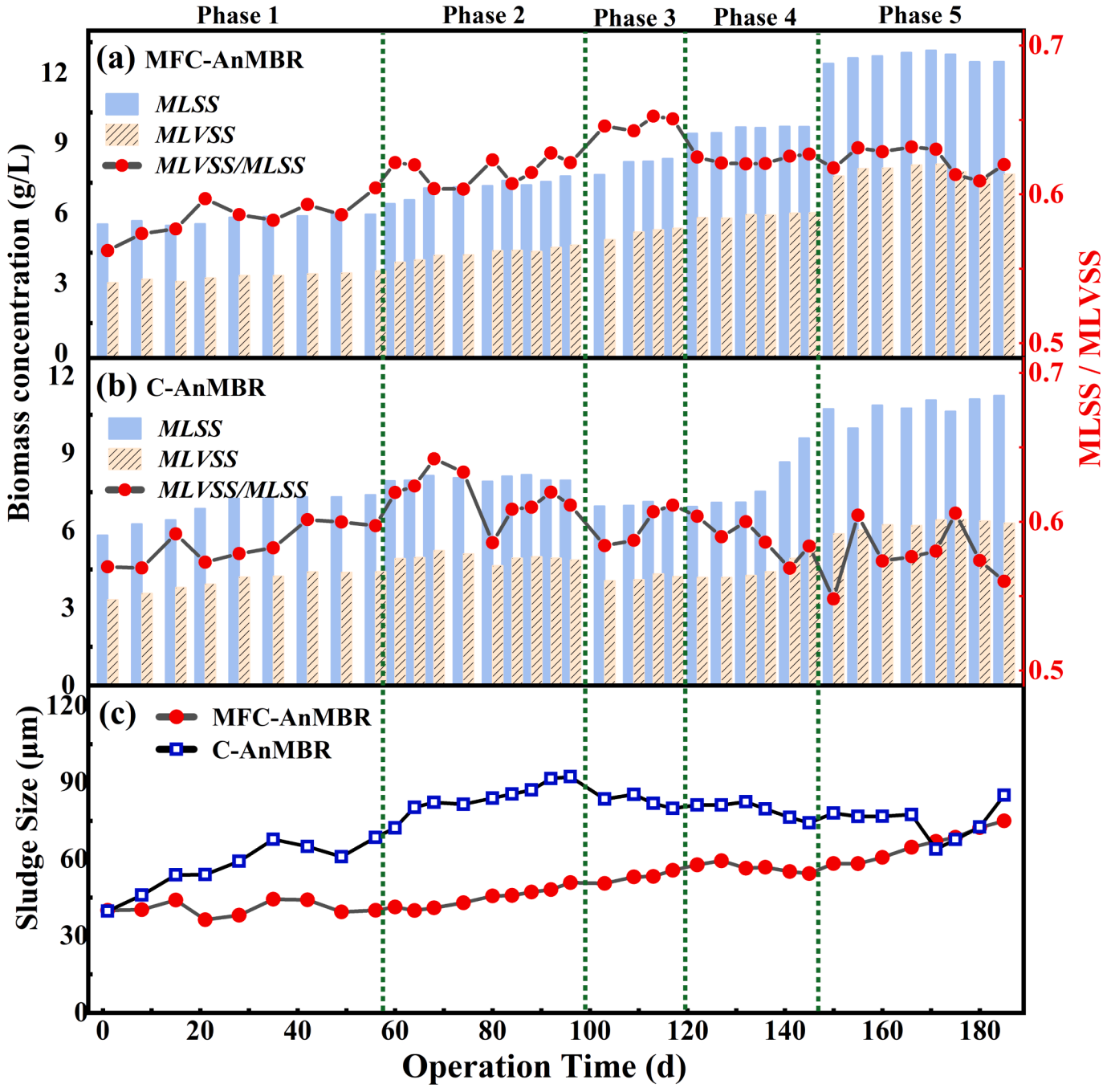

Fig. 5. Variations in (a) biomass of MFC-AnMBR, (b) biomass of C-AnMBR and (c) sludge size.

with microbial growth in MFC-AnMBR. A high organic load shock could cause a sudden biomass decline in C-AnMBR. Also, COD removal in C-AnMBR showed a significant decrease in Phases 3 and 4, indicating that the stability of the biomass was closely related to the system's stability. In addition, the MLVSS/MLSS ratio in the range of 0.6——0.8 stated the sludge under ideal conditions. In phases 1 and 2, the MLVSS/MLSS ratios in the two systems rose from 0.56 to 0.62, indicating a good sludge condition. In phases 3, 4 and 5, the MLVSS/MLSS ratio of MFC-AnMBR stabilized as the organic load increased, while that of C-AnMBR fluctuated up and down and finally dropped to around 0.57. This indicated that the bioelectric field helps adapt to the high organic load and ensures average growth and reproduction.

The change in sludge particle size is shown in Fig. 5c. In Phases 1 and 2, both systems exhibited a consistent upward trend, gradually transforming the initial particle size of 40 μm into 50 μm for MFC-AnMBR and 92 μm for C-AnMBR. Notably, the sludge particle size increased rapidly in C-AnMBR, associated with higher EPS concentrations, higher PN/PS (protein/polysaccharide) and lower absolute value of zeta potential (*detailed in section 3.3*). EPS played a crucial role in pelletization due to its surface charge ability and adhesion; higher PN/PS ratios also helped to stabilize the particle structure and facilitate sludge pelletization. As the absolute value of the zeta potential of EPS decreased, the flocculation equilibrium factor decreased, and the average flocculation particle size gradually increased [36]. However, intriguing observations unfolded as the experiment progressed into Phases 3, 4, and 5. When MFC-AnMBR continued its steady ascent, with the particle size growing from 50 μm to 75 μm, C-AnMBR took an unexpected turn, displaying a sudden downward trend. The particle size in C-AnMBR first decreased from 92 μm to 64 μm, only to rebound slightly to 85 μm thereafter. The sudden decrease in particle size during these phases can be attributed to the destabilization of the anaerobic system caused by the imposition of high organic load shocks. Overall, MFC-AnMBR effectively withstood

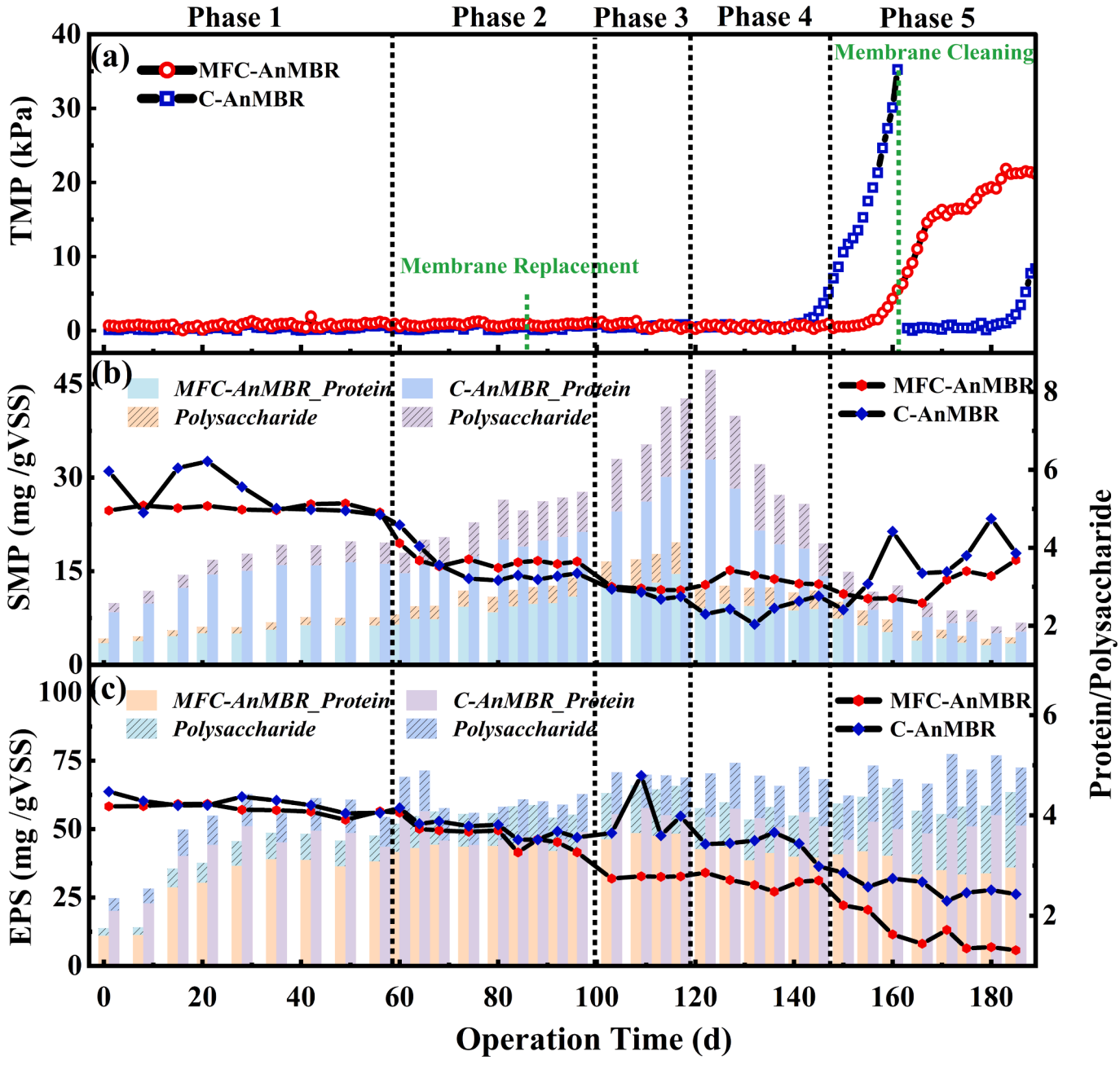

Fig. 6. Variations in (a) TMP, (b) SMP and (c) EPS in MFC-AnMBR and C-AnMBR.

the adverse effects of organic load shocks, maintaining a consistent increase in particle size.

3.3. Membrane fouling

3.3.1. TMP

TMP variations are shown in Fig. 6a. On day 86, both systems underwent simultaneous membrane replacements due to a membrane breakage incident in C-AnMBR. Within 114 days following the membrane replacement, C-AnMBR encountered two severe membrane fouling (TMP $>$ 35 kPa). One membrane cleaning was carried out between these two instances of severe membrane fouling. Interestingly, a reduction in the duration of TMP $<$ 1 (from 54 to 21 days) and membrane fouling cycle (from 21 to 18 days, shown in Fig. S1) was observed after the membrane cleaning. The shorter operating cycles of membrane modules meant the membrane fouling rate accelerated after cleaning. This was mainly because removing the pollutants in the membrane hole with strong adhesion by membrane cleaning alone was difficult, contributing to the more rapid formation of new pollutants [16]. These findings emphasized the self-accelerating nature of membrane fouling made the long-term stable operation of AnMBR quite challenging. In contrast, MFC-AnMBR showed an increase in TMP on day 70, about 14 days later than C-AnMBR. And the membrane in MFC-AnMBR was still in serviceable condition with a TMP of only 22.92 kPa at the end of the experiment, indicating that the bioelectric field extended the membrane fouling cycle by at least 40 days. Bioelectric field mitigated membrane fouling in AnMBR mainly due to reduced membrane pollutants concentration (such as SMP and EPS) and the change in microbial community structure (detailed in sections 3.3 and 3.4).

3.3.2. SMP and EPS

3.3.2.1. SMP and EPS concentration. Throughout the experiment, SMP concentrations in MFC-AnMBR and C-AnMBR were 6.21 $\pm$ 1.22 and 16.64 $\pm$ 3.44 mg/g_{VSS}, 11.17 $\pm$ 1.79 and 23.66 $\pm$ 3.31 mg/gvss, 17.69 $\pm$ 1.18 and 38.08 $\pm$ 4.05 mg/gvss, 12.16 $\pm$ 0.35 and 31.94 $\pm$ 9.27 mg/gvss, 6.26 $\pm$ 2.04 and 9.93 $\pm$ 2.81 mg/gvss, respectively (Fig. 6b). Interestingly, SMP concentrations in both reactors exhibited a consistent rise as the organic load increased in Phases 1–3. However, a significant decrease in SMP concentrations was observed in Phases 4–5, especially in C-AnMBR. Several factors contributed to this decline: firstly, the substantial proliferation of Firmicutes played a role in the degradation of SMP (*detailed in section 3.4*); and secondly, the rapid multiplication of microorganisms during Phases 4–5 decreased the F/M ratio. This shift caused SMP to be utilized as an energy source, supplementing cellular metabolic activity [35]. In addition, the results showed that the SMP concentration in the C-AnMBR was about twice as high as that in MFC-AnMBR, indicating that the bioelectric field reduced the SMP concentration to mitigate membrane fouling. The lower SMP concentration in MFC-AnMBR could be attributed to the following reasons: firstly, negatively charged substances (e.g., SMP and EPS) adsorbed by positively charged anodic carbon felts to form macromolecular precipitates [37]; and secondly, the bioelectric field enhanced microbial activity and thus facilitated the degradation of complex organic matter [38].

EPS variations were shown in Fig. 6c: EPS concentrations in MFC-AnMBR and C-AnMBR were 37.13 $\pm$ 13.24 and 45.94 $\pm$ 11.15 mg/gvss, 55.37 $\pm$ 2.09 and 62.39 $\pm$ 4.92 mg/gvss, 64.86 $\pm$ 1.14 and 69.73 $\pm$ 0.68 mg/gvss, 56.35 $\pm$ 2.26 and 70.12 $\pm$ 2.78 mg/gvss, 59.83 $\pm$ 3.13 and 71.10 $\pm$ 4.83 mg/gvss, respectively. Compared to C-AnMBR, the concentration of EPS in MFC-AnMBR decreased by 15.7 $\pm$ 10.9 %. The reason for the lower EPS concentration in MFC-AnMBR was consistent with that for the lower SMP concentration, i.e., anodic carbon felt adsorption and enhanced microbial activity by the bioelectric field. In addition, it was noteworthy that the EPS concentration in both reactors showed an increasing trend with increasing organic loads in Phases 1–3. Subsequently, a stable and slight decrease in EPS concentrations was observed in MFC-AnMBR, whereas increased in C-AnMBR. According to the reports, EPS secretion is a natural response of microorganisms to a new environment, by upregulating signalling molecules such as AI-2 or c-di-GMP when stimulated by increased organic loads [39,40]. Therefore, the variations in EPS concentration of MFC-AnMBR in Phases 4–5 indicated that the bioelectric field enhanced the ability of the AnMBR to adapt to the high organic loads environment, and thus, concentrations of EPS remained stable.

Furthermore, the PN/PS ratio of both reactors gradually decreased throughout the experiment, and the ratio of MFC-AnMBR decreased faster. It was worth noting that PN typically carried a positive charge resulting from amino hydrolysis, while PS bore a negative charge stemming from hydroxyl hydrolysis. Consequently, the absolute value of EPS zeta potential showed a negative correlation with the PN/PS ratio [41]. The lower PN/PS ratio in MFC-AnMBR resulted in a higher zeta potential, providing effective mitigation against membrane fouling (*detailed section 3.3.2.2*).

3.3.2.2. Zeta potential of SMP and EPS. To elucidate the relationship between changes in zeta potential of SMP and EPS and their impact on membrane fouling, simultaneous zeta potential measurements were conducted (Table S1). The results revealed an interesting phenomenon as EPS concentration increased, the absolute values of zeta potentials decreased. This observation corroborated the findings of Ding et al. [41]: higher EPS concentration corresponded to lower absolute values of zeta potential. Compared to C-AnMBR, higher absolute values of EPS zeta potentials were detected in MFC-AnMBR due to a lower EPS concentration and a lower PN/PS ratio, which was favourable to reducing the membrane fouling. Because many harmful substances such as SMP and EPS causing membrane fouling were adsorbed onto the membrane, the membrane surface became electronegative and thus repulsive to the negatively charged membrane pollutants. Therefore, the higher absolute value of EPS zeta potential in MFC-AnMBR was favourable to reducing the membrane fouling further caused by EPS. Furthermore, a minor zeta potential difference between EPS and SMP was observed in MFC-AnMBR. The more minor zeta potential difference indicated a stronger adhesion between EPS and SMP compared to C-AnMBR, which contributed to reducing the free SMP concentration in the reactor and alleviating membrane fouling caused by SMP.

3.4. Microbial community analysis

3.4.1. Mixed sludge

The distribution of community abundance at the phylum level is shown in Fig. 7a. *p_Actinobacteria, p_Bacteroidota, p_Firmicutes, p_Euryarchaeota, p_Halobacterota,* and *p_Proteobacteria* emerged as the dominant phyla throughout all phases in both reactors, collectively accounting for 60.0 % – 80.0 % of total abundance. Previous studies confirmed that *p_Actinobacteria, p_Bacteroidetes, p_Firmicutes,* and *p_Proteobacteria* were pivotal in anaerobic processes due to their ability to degrade diverse organic substances efficiently during fermentation [42,43]. Notably, *p_Actinobacteria* and *p_Bacteroides* excelled at converting particulate matter such as carbohydrates and proteins into dissolved substances. *P_Firmicutes* and *p_Proteobacteria* possessed the capability to break down various VFAs into acetate and hydrogen. The sheer abundance of these microorganisms ensured hydrolytic acidification of organic matter, leading to the exceptional COD removal observed in both reactors. *P_Halobacteria* and *p_Euryarchaea* were archaea containing various methanogenic bacteria, and their abundances in MFC-AnMBR and C-AnMBR were 2.5 % – 33.9 % and 12.7 % – 34.4 %, respectively, and their high abundance guaranteed efficient methane production. The significant presence of methanogens facilitated the conversion of acetate, methyl compounds, hydrogen, and carbon dioxide, thereby ensuring efficient methane production.

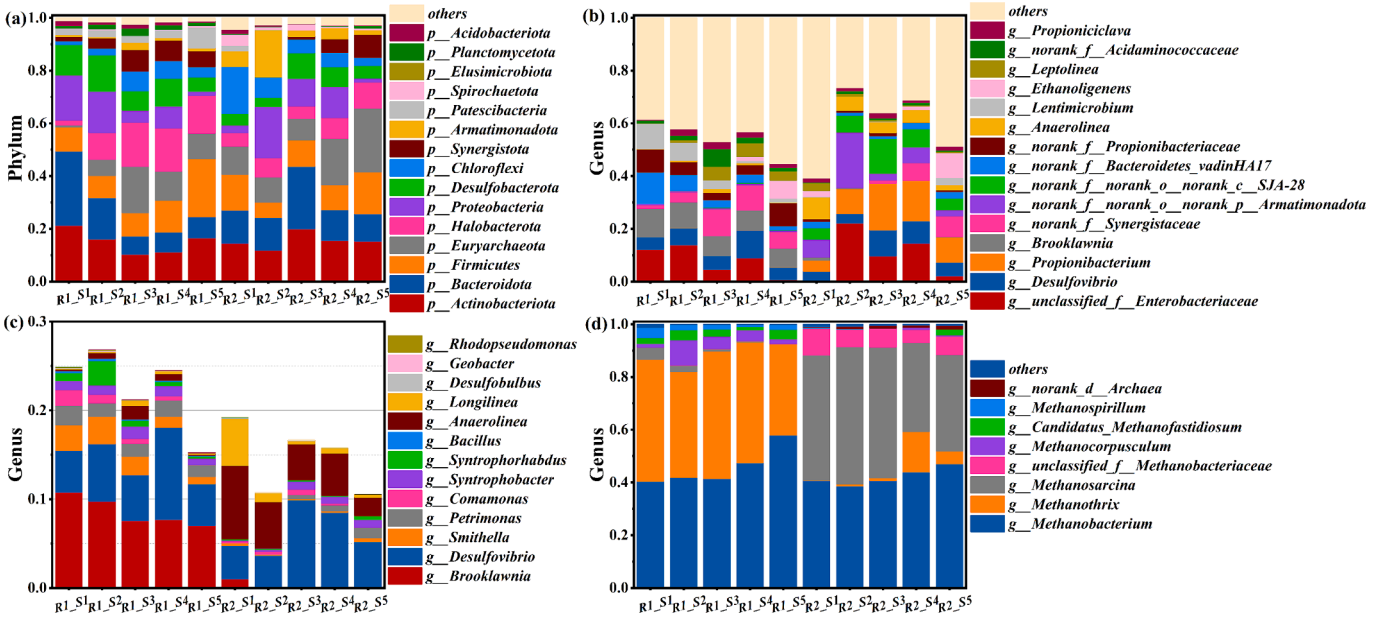

Fig. 7. Community abundance on (a) phylum, (b) genus Bacteria, (c) electroactive bacteria and (d) genus Archaea (R1 represent MFC-AnMBR, S1 represent Phase 1, and so on).

Notably, the abundance of archaea in MFC-AnMBR was lower than that in C-AnMBR in Phase 1 and Phase 5. Nevertheless, the methanogenic performance of MFC-AnMBR was consistently superior. This observation was attributed to the following: first, the bioelectric field enhanced the activity of the methanogens [44]; second, the bioelectric field enriched a higher abundance of electroactive bacteria (Fig. 7c), strengthening the interspecies electron transfer with the methanogens [16]; and third, the anodic carbon felt was also enriched with high abundance of methanogens (Fig. S2).

P_Synergistota deserved special attention. *P_Synergistota* were acid-forming bacteria known for their ability to produce short-chain VFAs and act as syntrophic acetate oxidizers. Recent studies have highlighted the electrochemical activity of Synergistota, enabling them to establish syntrophic metabolism with hydrogenotrophic methanogens such as *p_Methanobacterium* and participate in interspecies electron transfer. These findings suggested that *p_Synergistota* potentially played a crucial role in facilitating direct interspecies electron transfer interactions between microorganisms [45]. In Phases 1–4, higher abundance of *p_Synergistota* in MFC-AnMBR helped promote interspecies electrons in methanogens and improved methanogenic performance (1.7 % – 8.0 % in MFC-AnMBR and 0—5.18 % inC-AnMBR). Moreover, the significant decrease in abundance of *p_Synergistota* in MFC-AnMBR in Phase 5 was consistent with the trend of decreased methanogenic capacity, speculating that *p_Synergistota* may play an important role in the methanogenic process. This is evidenced by the sudden increase in abundance of *p_Synergistota* in C-AnMBR in Phases 4–5, which was in keeping with the trend of increased methanogenic capacity (detailed in section 3.2.3).

P_Firmicutes has been consistently reported to possess the ability to degrade complex organic compounds such as proteins and polysaccharides [43]. Their abundance reached a maximum of 22.8 % in MFC-AnMBR and 15.6 % in C-AnMBR during Phase 5, corresponding to a significant decrease in SMP. A previous study conducted by Hou et al. highlighted that *p_Firmicutes* contributed to the degradation of organic matter, subsequently reducing the concentration of SMP [38]. *P_Desulfobacterota* was noteworthy, known for its high electron transfer efficiency. In MFC-AnMBR, the abundance of *p_Desulfobacterota* ranged from 5.3 % to 13.9 %, higher than that in C-AnMBR (3.5 % – 9.6 %). This higher prevalence in MFC-AnMBR ensured stable operation of the bioelectric field and improve the electron transfer with methanogens.

Genus level analysis showed that the dominant genera were *g_unclassified_f_Enterobacteriaceae*, *g_Desulfovibrio*, *g_Propionibacterium* and *g_Brooklawnia* (Fig. 7b). *G_unclassified_f_Enterobacteriaceae*, belonged to *p_Proteobacteria* and was commonly found in wastewater remediation systems. They were known for their ability to break down micromolecular organic matter, thus assisting in eliminating various pollutants [46]. *G_Desulfovibrio* possessed polymeric conductivity and highly expressed genes involved in extracellular electron transfer, such as cytochromes, trichomes, and flagella. They were known to be electroactive bacteria and could directly transfer electrons [47]. Similarly, *g_Smithella* and *g_Syntrophobacter* belonging to *p_Desulfobacterota* were electroactive bacteria. They also specialized in working with methanogens through electron transfer [48]. The total abundance of these electroactive bacteria, all belonging to *p_Desulfobacterota*, was higher in MFC-AnMBR (5.3 % – 13.9 %) than in C-AnMBR (3.5 % – 9.6 %), which enhanced the electron transfer with methanogens and thus improved methanogenic performance. Both *g_Propionibacterium* and *g_Brooklawnia* belonged to *p_Actinibacteriota* and were known to produce VFAs. It was noteworthy that *g_Brooklawnia* dominated only in MFC-AnMBR (7.02 % – 10.76 %), while *g_Propionibacterium* dominated only in C-AnMBR (4.20 % – 17.62 %). Compared to *g_Propionibacterium*, *g_Brooklawnia* was shown to be electroactive and promoted methanogenesis by direct interspecific electron transfer with *g_Methanosaeta* [49]. Electroactive *g_Petrimonas* were also found in MFC-AnMBR (0.9 % – 2.1 % compared to 0 % – 0.8 % in C-AnMBR), and they were also hydrogen-producing bacteria, which can promote the production of more methane by interspecies hydrogen transfer with hydrogenotrophic methanogens [50]. Higher abundance of *g_Petrimonas* in MFC-AnMBR further improved methanogenic performance. These findings suggested that bioelectric fields exert a robust selective effect on microorganisms by influencing their community structure [47]. Remarkably, *g_Anaerolinea* was a filamentous microorganism that serves as a core or carrier in forming small sludge particles. *G_Anaerolinea* was found to be significantly positively correlated with a lot of EPS-forming genes [51]. In this study, the abundance of *g_Anaerolinea* ranged from 2.0 % to 8.1 % in C-AnMBR and from 0 % to 1.7 % in MFC-AnMBR. This dramatic difference suggested that the bioelectric field reduced the formation of EPS through its inhibitory effect on the abundance of *g_Anaerolinea*.

A taxonomic analysis of the archaeal microbial community is shown in Fig. 7d. In MFC-AnMBR, the dominant archaea were *g_Methanobacterium* (39.7 % – 58.3 %) and *g_Methanothrix* (34.2 % – 49.0 %).

In contrast, C-AnMBR showed a higher presence of hybrid multi-pathway *g_Methanosarcina* (34.5 % – 52.2 %), while hydrogenotrophic *g_Methanobacterium* (38.6 % – 47.0 %) were less abundant. *G_Methanobacterium* exhibited an increasing trend in relative abundance with increasing organic load in two reactors, ultimately becoming the dominant methanogen, especially in MFC-AnMBR. This shift can be attributed to the higher substrate utilization, growth rate, and cell production of hydrogenotrophic methanogens compared to acetoclastic methanogens when exposed to high organic loads [52]. Additionally, *g_Methanobacterium* was a type of methanogen capable of extracellular respiration, directly capturing electrons from electroactive bacteria such as *g_Desulfovibrio* and *g_Synergistota* to convert CO_2 to methane [47,53]. The enrichment of more electroactive bacteria and *g_Methanobacterium* in MFC-AnMBR was responsible for its higher methane production and content. In addition, it was worth noting that *g_Methanothrix* (formally *g_Methanosaeta*) and *g_Methanosarcina*, the other major methanogens in MFC-AnMBR and C-AnMBR, respectively, can use the acetate decarboxylation pathway for acetate isomerisation to produce methane [54,55]. The dominance of *g_Methanosaeta* in MFC-AnMBR may be related to the facilitation of direct interspecies electron transfer (DIET) brought by bioelectric fields, as these species can directly accept electrons from electroactive bacteria, especially *g_Brooklawnia* [56]. In summary, BES's presence dramatically changed the microbial community's structure. It enhanced methane production by selecting and promoting the growth of methanogens that can engage in a mutualistic relationship with electroactive bacteria.

3.4.2. Biomass on membrane

The change in microbial abundance on the membrane is shown in Fig. 8. Similar to mixed sludge in the reactors, the top six dominant phyla all included *p_Halobacterota, p_Bacteroidota, p_Euryarchaeota, p_Firmicutes* and *p_Actinobacteria*, with a total abundance of 52.0 % – 68.0 % in all phases. As above, *p_Halobacter* and *p_Euryarchaea* contained various methanogens and had a large proportion on the membrane with abundances of 25.6 % – 38.0 % and 23.1 % – 51.8 % in MFC-AnMBR and C-AnMBR, respectively. Furthermore, their abundance was maximum when membrane fouling was most serious in both reactors and minimum after membrane cleaning in C-AnMBR. This may be related to the unique characteristics of the archaeal cell envelope that contributed to the persistence of these organisms on the membrane surface [57], thus promoting membrane fouling. Genus level analysis showed that *g_Methanocorpusculum* was the main methanogen that exacerbated the membrane fouling, and its abundance was proportional to the membrane fouling. Its abundance was as high as 20.8 % in MFC-AnMBR (Phase 5, TMP≈21.5 kPa) and 33.7 % in C-AnMBR (TMP > 35 kPa) when the membrane fouling was most profound. *P_Bacteroidota* was also a vital phylum causing membrane fouling [58] and was detected in relatively high abundance in two reactors. Gao et al. reported that the formation of *p_Bacteroidota* colonies on the membrane surface was favoured by more EPS release [59]. Thus, the much higher abundance of *p_Bacteroidota* in C-AnMBR (10.8 % – 26.6 %) than in MFC-AnMBR (6.3 % – 12.9 %) contributed to the accelerated membrane fouling. As Cheng et al. reported that *p_Firmicutes* had the property of accelerating biofouling in AnMBR, significant amounts of *p_Firmicutes* on the membrane were found (4.8 % – 7.3 % in MFC-AnMBR and 6.2 % – 12.8 % in C-AnMBR) [20]. Interestingly, however, *p_Firmicutes* was found to be minimum in two reactors when membrane fouling was most profound. Therefore, *p_Firmicutes* may act as pioneer bacteria in the initial formation of the filter cake layer due to their strong ability to grow on the membrane [60]. Hence, the bioelectric fields helped to mitigate membrane fouling by inhibiting the growth of the above membrane fouling-causing bacteria. Additionally, a high abundance of *p_Actinobacteria* was detected in MFC-AnMBR (4.0 % – 13.5 %), while only 2.9 % – 4.1 % in C-AnMBR. *P_Actinobacteria* could degrade organic and inorganic pollutants due to their ability to produce a wide range of extracellular hydrolases, e.g. by creating cellulases and chitinases to degrade various organic substances such as cellulose, polysaccharides, proteins, fats, organic acids and humus [61]. Thus, two times more abundance of *p_Actinobacteria* in MFC-AnMBR than in C-AnMBR contributed to the membrane fouling mitigation.

4. Conclusion

This work investigated system performance and membrane fouling of MFC-AnMBR treating SW at different organic loads in long-term operation. Results indicated that for C-AnMBR, the sudden increase in organic loads shocked anaerobic microorganisms, temporarily reducing the system performance (mainly methane production) and the operation stability (including pH, biomass and particle size). Nevertheless, thanks to the bioelectric field, MFC-AnMBR withstood high organic load shocks, and excelled in system start-up, pollutant removal, methane production and system stability. The bioelectric field promoted less SMP and EPS, increased the absolute values of EPS zeta potentials at various organic loads. This helped extend the membrane life cycle by at least 40 days in MFC-AnMBR. Microbiological analysis showed that the dominance of aceticlastic methanogens shifted to hydrogenotrophic methanogens with increasing organic loads. Meanwhile, the methane content rose, a trend facilitated by the bioelectric field. Additionally, the bioelectric field had a selective effect on microorganisms, as evidenced by the more electroactive bacteria (*g_Desulfovibrio*, *g_Petrimonas*, and *g_Brooklawnia*) and methanogens capable of electron transfer (*g_Methanobaterium* and *g_Methanothix*) in MFC-AnMBR. Furthermore, analysis of microbial community attached on the membrane showed that *g_Methanocorpusculum* was the key fouling-causing bacterium and *p_Actinobacteria* were fouling-reducing bacteria. The bioelectric field decreased the abundance of *Methanocorpusculum* and increased the abundance of Actinobacteria to mitigate membrane fouling. These results showed that the bioelectric field could effectively improve the operational stability, COD removal, and methane production and relieve membrane fouling of AnMBR in the long-term operation. However, this

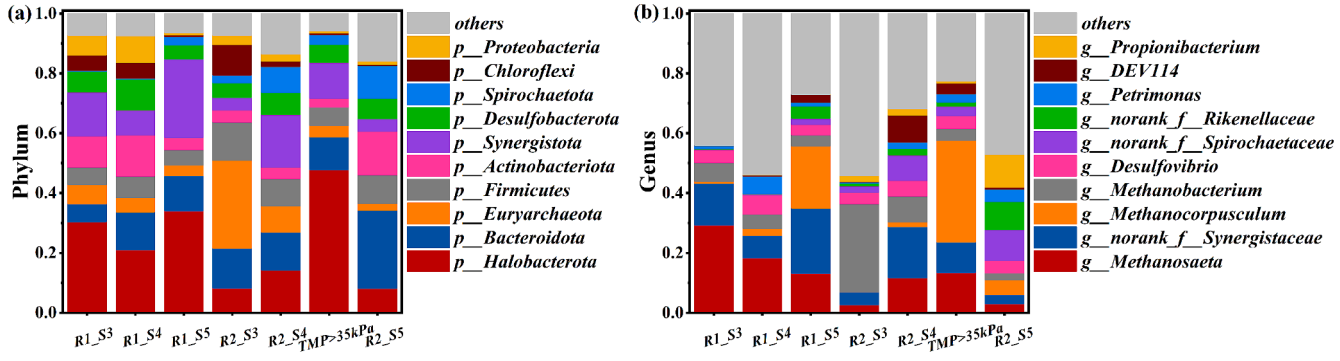

Fig. 8. Community abundance on (a) phylum and (b) genus (R1 represent MFC-AnMBR, S1 represent Phase 1, and so on).

MFC-AnMBR system was operated on a lab scale in this study. A pilot or full-scale operation is needed to achieve the widespread application of MFC-AnMBR technology.

CRediT authorship contribution statement

Haojie Huang: Writing – original draft, Methodology, Investigation. **Xinbo Zhang:** Writing – review & editing, Supervision, Project administration, Investigation. **Qing Du:** Formal analysis, Data curation. **Fu Gao:** Methodology, Formal analysis. **Zhiwen Wang:** Methodology, Data curation. **Guangxue Wu:** Investigation, Formal analysis. **Wenshan Guo:** Writing – review & editing, Investigation. **Huu Hao Ngo:** Writing – review & editing, Supervision, Investigation.

Declaration of competing interest

The authors declare that they have no known competing financial interests or personal relationships that could have appeared to influence the work reported in this paper.

Data availability

Data will be made available on request.

Acknowledgements

This research was supported by Tianjin Municipal Science and Technology Bureau of China (Project No.20JCZDJC00380 and 18PTZWHZ00140).

Appendix A. Supplementary data

Supplementary data to this article can be found online at https://doi.org/10.1016/j.cej.2024.152772.

References

[1] D. Garcia, E. Posadas, C. Grajeda, S. Blanco, S. Martinez-Paramo, G. Acien, P. Garcia-Encina, S. Bolado, R. Munoz, Comparative evaluation of piggery wastewater treatment in algal-bacterial photobioreactors under indoor and outdoor conditions, Bioresour. Technol. 245 (Pt A) (2017) 483–490, https://doi.org/10.1016/j.biortech.2017.08.135.

[2] D.L. Cheng, H.H. Ngo, W.S. Guo, S.W. Chang, D.D. Nguyen, S.M. Kumar, Microalgae biomass from swine wastewater and its conversion to bioenergy, Bioresour. Technol. 275 (2019) 109–122, https://doi.org/10.1016/j.biortech.2018.12.019.

[3] N. Wang, Y. Feng, Y. Li, L. Zhang, J. Liu, N. Li, W. He, Effects of ammonia on electrochemical active biofilm in microbial electrolysis cells for synthetic swine wastewater treatment, Water Res. 219 (2022) 118570, https://doi.org/10.1016/j.watres.2022.118570.

[4] M. Dolatabadi, S. Ahmadzadeh, Microplastics pollution in the aquatic environment: problems and challenges, J. Environm. Health Sustain. Developm. (2020), https://doi.org/10.24200/amecj.v6.i02.236.

[5] G.D. Noudeh, M. Asdaghi, N.D. Noudeh, M. Dolatabadi, S. Ahmadzadeh, Response surface modeling of ceftriaxone removal from hospital wastewater, Environ. Monit. Assess. 195 (1) (2023) 217, https://doi.org/10.1007/s10661-022-10808-z.

[6] H. Deng, H. Ren, J. Fan, K. Zhao, C. Hu, J. Qu, Membrane fouling mitigation by coagulation and electrostatic repulsion using an electro-AnMBR in kitchen wastewater treatment, Water Res. 222 (2022) 118883, https://doi.org/10.1016/j.watres.2022.118883.

[7] Y.H. Pu, J.L. Tang, T. Zeng, Y.S. Hu, J.X. Yang, X.C. Wang, J. Huang, A. Abomohra, Pollutant removal and energy recovery from swine wastewater using anaerobic membrane bioreactor: a comparative study with up-flow anaerobic sludge blanket, Water. 14 (15) (2022) 2438, https://doi.org/10.3390/w14152438.

[8] W. Liu, X. Song, X. Ding, R. Xia, X. Lin, G. Li, L.D. Nghiem, W. Luo, Antibiotic removal from swine farming wastewater by anaerobic membrane bioreactor: Role of hydraulic retention time, J. Membr. Sci. 677 (2023) 121629, https://doi.org/10.1016/j.memsci.2023.121629.

[9] H.H. Xinbo Zhang, Du. Qing, Fu. Gao, Z. Wang, Wu. Guangxue, W. Guo, H.H. Ngo, Performance of a recirculated biogas-sparging anaerobic membrane bioreactor system for treating synthetic swine wastewater containing sulfadiazine antibiotic, Chem. Eng. J. 476 (2024) 146735, https://doi.org/10.1016/j.cej.2023.146735.

[10] C. Sun, Q. Du, X. Zhang, Z. Wang, J. Zheng, Q. Wu, Z. Li, T. Long, W. Guo, H. H. Ngo, Role of spent coffee ground biochar in an anaerobic membrane bioreactor for treating synthetic swine wastewater, J. Water Process Eng. 49 (2022) 102981, https://doi.org/10.1016/j.jwpe.2022.102981.

[11] D. Cheng, H.H. Ngo, W. Guo, S.W. Chang, D.D. Nguyen, Q.A. Nguyen, J. Zhang, S. Liang, Improving sulfonamide antibiotics removal from swine wastewater by supplying a new pomelo peel derived biochar in an anaerobic membrane bioreactor, Bioresour. Technol. 319 (2021) 124160, https://doi.org/10.1016/j.biortech.2020.124160.

[12] M. Dolatabadi, R. Akbarpour, S. Ahmadzadeh, Catalytic ozonation process using ZnO/Fe2O3 nanocomposite for efficient removal of captopril from aqueous solution, Anal. Methods Environm. Chem. J. 5 (03) (2022) 31–39, https://doi.org/10.1080/03601234.2023.2247943.

[13] M. Dolatabadi, M.H. Ehrampoush, M. Pournamdari, A.A. Ebrahimi, H. Fallahzadeh, S. Ahmadzadeh, Catalytic electrodes' characterization study serving polluted water treatment: environmental healthcare and ecological risk assessment, J. Environ. Sci. Health B 58 (9) (2023) 594–602, https://doi.org/10.1080/03601234.2023.2247943.

[14] M. Maaz, M. Yasin, M. Aslam, G. Kumar, A.E. Atabani, M. Idrees, F. Anjum, F. Jamil, R. Ahmad, A.L. Khan, G. Lesage, M. Heran, J. Kim, Anaerobic membrane bioreactors for wastewater treatment: Novel configurations, fouling control and energy considerations, Bioresour. Technol. 283 (2019) 358–372, https://doi.org/10.1016/j.biortech.2019.03.061.

[15] M. Dolatabadi, T. Świergosz, C. Wang, S. Ahmadzadeh, Accelerated degradation of groundwater-containing malathion using persulfate activated magnetic Fe3O4/graphene oxide nanocomposite for advanced water treatment, Arab. J. Chem. 16 (1) (2023) 104424, https://doi.org/10.1016/j.arabjc.2022.104424.

[16] Y. Hao, X. Zhang, Q. Du, H. Wang, H.H. Ngo, W. Guo, Y. Zhang, T. Long, L. Qi, A new integrated single-chamber air-cathode microbial fuel cell - Anaerobic membrane bioreactor system for improving methane production and membrane fouling mitigation, J. Membr. Sci. 655 (2022) 120591, https://doi.org/10.1016/j.memsci.2022.120591.

[17] M. Dolatabadi, S. Ahmadzadeh, Catalytic ozonation process using modified activated carbon as a cataly st for the removal of sarafloxacin antibiotic from aqueous solutions, Anal. Methods Environm. Chem. J. 6 (02) (2023) 31–41, https://doi.org/10.24200/amecj.v6.i02.236.

[18] M. Dolatabadi, A. Kheirieh, M. Yoosefian, S. Ahmadzadeh, Hydroxyzine removal from the polluted aqueous solution using the hybrid treatment process of electrocoagulation and adsorption; optimization, and modeling, Appl. Water Sci. 12 (11) (2022) 254, https://doi.org/10.1007/s13201-022-01780-7.

[19] M. Dolatabadi, M.H. Ehrampoush, M. Pournamdari, A.A. Ebrahimi, H. Fallahzadeh, S. Ahmadzadeh, Simultaneous electrochemical degradation of pesticides from the aqueous environment using Ti/SnO2–Sb2O3/PbO2/Bi electrode; process modeling and mechanism insight, Chemosphere 311 (2023) 137001, https://doi.org/10.1016/j.chemosphere.2022.137001.

[20] D. Cheng, H.H. Ngo, W. Guo, Y. Liu, S.W. Chang, D.D. Nguyen, L.D. Nghiem, J. Zhou, B. Ni, Anaerobic membrane bioreactors for antibiotic wastewater treatment: Performance and membrane fouling issues, Bioresour. Technol. 267 (2018) 714–724, https://doi.org/10.1016/j.biortech.2018.07.133.

[21] M. Dolatabadi, M.H. Ehrampoush, M. Pournamdari, A.A. Ebrahimi, H. Fallahzadeh, S. Ahmadzadeh, Enhanced electrocatalytic elimination of fenitrothion, trifluralin, and chlorothalonil from groundwater and industrial wastewater using modified Cu-PbO2 electrode, J. Mol. Liq. 379 (2023) 121706, https://doi.org/10.1016/j.molliq.2023.121706.

[22] Y. Liu, X. Cao, J. Zhang, Z. Fang, H. Zhang, X. Gao, X. Li, The use of a self-generated current in a coupled MFC-AnMBR system to alleviate membrane fouling, Chem. Eng. J. 442 (2022) 136090, https://doi.org/10.1016/j.cej.2022.136090.

[23] M.H. McCrady, Standard methods for the examination of water and waste-water, Am. J. Public Health Nations Health. 56 (4) (1966) 684, https://doi.org/10.2105/AJPH.56.4.684-a.

[24] X. Lu, G. Zhen, Y. Liu, T. Hojo, A.L. Estrada, Y.-Y. Li, Long-term effect of the antibiotic cefalexin on methane production during waste activated sludge anaerobic digestion, Bioresour. Technol. 169 (2014) 644–651, https://doi.org/10.1016/j.biortech.2014.07.056.

[25] T. Magoč, S.L. Salzberg, FLASH: fast length adjustment of short reads to improve genome assemblies, Bioinformatics 27 (21) (2011) 2957–2963, https://doi.org/10.1093/bioinformatics/btr507.

[26] R.C. Edgar, UPARSE: highly accurate OTU sequences from microbial amplicon reads, Nat. Methods 10 (10) (2013) 996–998, https://doi.org/10.1038/nmeth.2604.

[27] Q. Wang, G.M. Garrity, J.M. Tiedje, J.R. Cole, Naïve bayesian classifier for rapid assignment of rrna sequences into the new bacterial taxonomy, Appl. Environ. Microbiol. 73 (16) (2007) 5261–5267, https://doi.org/10.1128/aem.00062-07.

[28] G.M.F. Pierangeli, R.A. Ragio, R.F. Benassi, G.B. Gregoracci, E.L. Subtil, Pollutant removal, electricity generation and microbial community in an electrochemical membrane bioreactor during co-treatment of sewage and landfill leachate, J. Environ. Chem. Eng. 9 (5) (2021) 106205, https://doi.org/10.1016/j.jece.2021.106205.

[29] J. Chen, T. Wang, K. Zhang, H. Luo, W. Chen, Y. Mo, Z. Wei, The fate of antibiotic resistance genes (ARGs) and mobile genetic elements (MGEs) from livestock wastewater (dominated by quinolone antibiotics) treated by microbial fuel cell (MFC), Ecotoxicol Environ Saf. 218 (2021) 112267, https://doi.org/10.1016/j.ecoenv.2021.112267.

[30] A.F. Aili Hamzah, M.H. Hamzah, H. Che Man, N.S. Jamali, S.I. Siajam, M.H. Ismail, Effect of organic loading on anaerobic digestion of cow dung: Methane production and kinetic study, Heliyon. 9 (6) (2023) e16791.

[31] S.P. Tan, H.F. Kong, M.J.K. Bashir, P.K. Lo, C.-D. Ho, C.A. Ng, Treatment of palm oil mill effluent using combination system of microbial fuel cell and anaerobic

membrane bioreactor, Bioresour. Technol. 245 (2017) 916–924, https://doi.org/10.1016/j.biortech.2017.08.202.
[32] R. Moradi, S.M. Monfared, Y. Amini, A. Dastbaz, Vacuum enhanced membrane distillation for trace contaminant removal of heavy metals from water by electrospun PVDF/TiO2 hybrid membranes, Korean J. Chem. Eng. 33 (7) (2016) 2160–2168, https://doi.org/10.1007/s11814-016-0081-y.
[33] Y. Sun, A. ter Heijne, H. Rijnaarts, W.-S. Chen, The effect of anode potential on electrogenesis, methanogenesis and sulfidogenesis in a simulated sewer condition, Water Res. 226 (2022) 119229, https://doi.org/10.1016/j.watres.2022.119229.
[34] C. Wang, S. Nakakoji, T.C.A. Ng, P. Zhu, R. Tsukada, M. Tatara, H.Y. Ng, Acclimatizing waste activated sludge in a thermophilic anaerobic fixed-bed biofilm reactor to maximize biogas production for food waste treatment at high organic loading rates, Water Res. 242 (2023) 120299, https://doi.org/10.1016/j.watres.2023.120299.
[35] G. Balcıoğlu, G. Yilmaz, Z.B. Gönder, Evaluation of anaerobic membrane bioreactor (AnMBR) treating confectionery wastewater at long-term operation under different organic loading rates: Performance and membrane fouling, Chem. Eng. J. 404 (2021) 126261, https://doi.org/10.1016/j.cej.2020.126261.
[36] Z. Li, P. Lu, D. Zhang, G. Chen, S. Zeng, Q. He, Population balance modeling of activated sludge flocculation: Investigating the influence of Extracellular Polymeric Substances (EPS) content and zeta potential on flocculation dynamics, Sep. Purif. Technol. 162 (2016) 91–100, https://doi.org/10.1016/j.seppur.2016.02.011.
[37] X. Xiang, J. Bai, W. Gu, S. Peng, K. Shih, Mechanism and application of modified bioelectrochemical system anodes made of carbon nanomaterial for the removal of heavy metals from soil, Chemosphere 345 (2023) 140431, https://doi.org/10.1016/j.chemosphere.2023.140431.
[38] B. Hou, X. Liu, R. Zhang, Y. Li, P. Liu, J. Lu, Investigation and evaluation of membrane fouling in a microbial fuel cell-membrane bioreactor systems (MFC-MBR), Sci. Total Environ. 814 (2022) 152569, https://doi.org/10.1016/j.scitotenv.2021.152569.
[39] S. Sun, X. Liu, B. Ma, C. Wan, D.-J. Lee, The role of autoinducer-2 in aerobic granulation using alternating feed loadings strategy, Bioresour. Technol. 201 (2016) 58–64, https://doi.org/10.1016/j.biortech.2015.11.032.
[40] J.Y. Wang, B. Zhao, Q. An, Q. Dan, J.S. Guo, Y.P. Chen, The acceleration of aerobic sludge granulation by alternating organic loading rate: Performance and mechanism, J. Environ. Manage. 347 (2023) 119047, https://doi.org/10.1016/j.jenvman.2023.119047.
[41] Y. Ding, Y. Tian, Z. Li, W. Zuo, J. Zhang, A comprehensive study into fouling properties of extracellular polymeric substance (EPS) extracted from bulk sludge and cake sludge in a mesophilic anaerobic membrane bioreactor, Bioresour. Technol. 192 (2015) 105–114, https://doi.org/10.1016/j.biortech.2015.05.067.
[42] D.L. Cheng, H.H. Ngo, W.S. Guo, S.W. Chang, D.D. Nguyen, S.M. Kumar, B. Du, Q. Wei, D. Wei, Problematic effects of antibiotics on anaerobic treatment of swine wastewater, Bioresour. Technol. 263 (2018) 642–653, https://doi.org/10.1016/j.biortech.2018.05.010.
[43] A. Aziz, A. Sengar, F. Basheer, I.H. Farooqi, M.H. Isa, Anaerobic digestion in the elimination of antibiotics and antibiotic-resistant genes from the environment – A comprehensive review, J. Environ. Chem. Eng. 10 (1) (2022) 106423, https://doi.org/10.1016/j.jece.2021.106423.
[44] A. Dhanda, S. Das, B.K. Dubey, M.M. Ghangrekar, Anodic inoculum pre-treatment with green strategies for enhanced electron shuttling and suppressing methanogens in microbial fuel cell: a review, Biores. Technol. Rep. 24 (2023) 101593, https://doi.org/10.1016/j.biteb.2023.101593.
[45] M. Shao, C. Zhang, X. Wang, N. Wang, Q. Chen, G. Cui, Q. Xu, Co-digestion of food waste and hydrothermal liquid digestate: Promotion effect of self-generated hydrochars, Environ. Sci. Tech. 15 (2023) 100239, https://doi.org/10.1016/j.ese.2023.100239.
[46] X. Zhu, L. Wang, X. Zhang, M. He, D. Wang, Y. Ren, H. Yao, J. net Victoria Ngegla, H. Pan, Effects of different types of anthropogenic disturbances and natural wetlands on water quality and microbial communities in a typical black-odor river, Ecol. Ind. 136 (2022) 108613, https://doi.org/10.1016/j.ecolind.2022.108613.
[47] S. Zheng, M. Li, Y. Liu, F. Liu, Desulfovibrio feeding Methanobacterium with electrons in conductive methanogenic aggregates from coastal zones, Water Res. 202 (2021) 117490, https://doi.org/10.1016/j.watres.2021.117490.
[48] J. Du, Q. Yin, X. Zhou, Q. Guo, G. Wu, Distribution of extracellular amino acids and their potential functions in microbial cross-feeding in anaerobic digestion systems, Bioresour. Technol. 360 (2022) 127535, https://doi.org/10.1016/j.biortech.2022.127535.
[49] W. Wu, S.G. Arhin, H. Sun, Z. Li, Z. Yang, G. Liu, W. Wang, Facilitated CO biomethanation by exogenous materials via inducing specific methanogenic pathways, Chem. Eng. J. 460 (2023) 141736, https://doi.org/10.1016/j.cej.2023.141736.
[50] R. Sun, A. Zhou, J. Jia, Q. Liang, Q. Liu, D. Xing, N. Ren, Characterization of methane production and microbial community shifts during waste activated sludge degradation in microbial electrolysis cells, Bioresour. Technol. 175 (2015) 68–74, https://doi.org/10.1016/j.biortech.2014.10.052.
[51] Y. Zhao, B. Jiang, X. Tang, S. Liu, Metagenomic insights into functional traits variation and coupling effects on the anammox community during reactor start-up, Sci. Total Environ. 687 (2019) 50–60, https://doi.org/10.1016/j.scitotenv.2019.05.491.
[52] W.A. Botello Suarez, J. da Silva Vantini, R.M. Duda, P.F. Giachetto, L.C. Cintra, M. I. Tiraboschi Ferro, R.A. de Oliveira, Predominance of syntrophic bacteria, Methanosaeta and Methanoculleus in a two-stage up-flow anaerobic sludge blanket reactor treating coffee processing wastewater at high organic loading rate, Bioresour. Technol. 268 (2018) 158–168, https://doi.org/10.1016/j.biortech.2018.06.091.
[53] T. Wang, C. Li, L. Wang, M. Zhou, J. Ning, X. Pan, G. Zhu, Anaerobic digestion of sludge filtrate assisted by symbionts of short chain fatty acid-oxidation syntrophs and exoelectrogens: Process performance, methane yield and microbial community, J. Hazard. Mater. 384 (2020) 121222, https://doi.org/10.1016/j.jhazmat.2019.121222.
[54] C. Liu, D. Sun, Z. Zhao, Y. Dang, D.E. Holmes, Methanothrix enhances biogas upgrading in microbial electrolysis cell via direct electron transfer, Bioresour. Technol. 291 (2019) 121877, https://doi.org/10.1016/j.biortech.2019.121877.
[55] Y. Yan, J. Zhang, L. Tian, X. Yan, L. Du, A. Leininger, M. Zhang, N. Li, Z.J. Ren, X. Wang, DIET-like mutualism of Geobacter and methanogens at specific electrode potential boosts production of both methane and hydrogen from propionate, Water Res. 235 (2023) 119911, https://doi.org/10.1016/j.watres.2023.119911.
[56] D. Kalantzis, I. Daskaloudis, T. Lacoere, A.S. Stasinakis, D.F. Lekkas, J. De Vrieze, M.S. Fountoulakis, Granular activated carbon stimulates biogas production in pilot-scale anaerobic digester treating agro-industrial wastewater, Bioresour. Technol. 376 (2023) 128908, https://doi.org/10.1016/j.biortech.2023.128908.
[57] K. Calderon, B. Rodelas, N. Cabirol, J. Gonzalez-Lopez, A. Noyola, Analysis of microbial communities developed on the fouling layers of a membrane-coupled anaerobic bioreactor applied to wastewater treatment, Bioresour. Technol. 102 (7) (2011) 4618–4627, https://doi.org/10.1016/j.biortech.2011.01.007.
[58] C. Juntawang, C. Rongsayamanont, E. Khan, Entrapped cells-based-anaerobic membrane bioreactor treating domestic wastewater: Performances, fouling, and bacterial community structure, Chemosphere 187 (2017) 147–155, https://doi.org/10.1016/j.chemosphere.2017.08.113.
[59] W.J.J. Gao, H.J. Lin, K.T. Leung, B.Q. Liao, Influence of elevated pH shocks on the performance of a submerged anaerobic membrane bioreactor, Process Biochem. 45 (8) (2010) 1279–1287, https://doi.org/10.1016/j.procbio.2010.04.018.
[60] K. Takada, T. Shiba, T. Yamaguchi, Y. Akane, Y. Nakayama, S. Soda, D. Inoue, M. Ike, Cake layer bacterial communities during different biofouling stages in full-scale membrane bioreactors, Bioresour. Technol. 259 (2018) 259–267, https://doi.org/10.1016/j.biortech.2018.03.051.
[61] K. Boubekri, A. Soumare, I. Mardad, K. Lyamlouli, Y. Ouhdouch, M. Hafidi, L. Kouisni, Multifunctional role of Actinobacteria in agricultural production sustainability: A review, Microbiol. Res. 261 (2022) 127059, https://doi.org/10.1016/j.micres.2022.127059.